Journal of
Marine Science and Engineering

MDPI

Article

Not a Rolling Stone: On Dragging a Stone Weight-Anchor on the Seabed

Yoav Me-Bar [1,*], Ayelet Miller [2], Baruch Ephraim Karlin [3] and Deborah Cvikel [1,2]

[1] The Leon Recanati Institute for Maritime Studies, University of Haifa, Haifa 3498838, Israel; dcvikel@research.haifa.ac.il
[2] Department of Maritime Civilizations, University of Haifa, Haifa 3498838, Israel
[3] Independent Researcher, Haifa 3452413, Israel; bekarlin@gmail.com
* Correspondence: ymebar@yahoo.com

Abstract: The force required to drag a stone anchor over several types of surfaces was measured, recorded, and analyzed. It was found that the force involved in the movement of the anchor over the various surfaces cannot be described just by the sliding solids theory, but it involves several additional physical processes, such as increasing the sand shear strength by the pressure the anchor applies on the sand under it; the sinking of the anchor into the saturated sand; shearing the sand in front of the moving anchor and accelerating it to the velocity of the anchor; accumulating sand in front of the anchor, thus adding to the pulled mass; and moving some of the accumulated sand sideways. In many instances, the beginning of the anchor movement involves the liquefaction of the sand under it, thus enabling the relatively easier sliding of the anchor. In addition, movement over rocky surfaces, encountering the irregularities that abound on such surfaces, also differs from classic sliding friction theory. In several situations, the use of an effective coefficient of friction, combining all the processes, can serve to obtain approximate values of the required forces.

Keywords: friction; coefficient of friction; dragging on sand; liquefaction; sand shear strength; stone anchor

Citation: Me-Bar, Y.; Miller, A.; Karlin, B.E.; Cvikel, D. Not a Rolling Stone: On Dragging a Stone Weight-Anchor on the Seabed. *J. Mar. Sci. Eng.* **2024**, *12*, 248. https://doi.org/10.3390/jmse12020248

Academic Editor: Vincenzo Crupi

Received: 26 December 2023
Revised: 20 January 2024
Accepted: 26 January 2024
Published: 30 January 2024

1. Introduction

Stone weight-anchors were in widespread use during the Bronze Age (ca. 3500–1150 BCE) and Iron Age (ca. 1200–500 BCE), all around the eastern Mediterranean [1–3]). The locations where they were found mark anchorages and wreck-sites along the ancient maritime trade routes. Occasionally, they were also used on land for secondary uses [1,2,4] Many such anchors have been found, recorded, and cataloged [5,6], primarily to try and relate them to specific cultures and locations by typological analysis [7–9]. However, very little was recorded on their technological aspects. The late Professor Kahanov raised the question: 'What is the holding power of a Bronze Age stone anchor?' His question was partly answered by the work carried out by [10], who performed an extensive test series of measuring the force required to drag anchors of various sizes over a sandy or rocky sea bottom. The results enabled the estimation of the sizes of the ships that plied the Mediterranean during the Bronze and Iron Ages using these anchors. The present article is based on the results of that project, and deals with the various shapes (but not of the amplitudes) of the measured force history plots and with the analyses of the physical processes at the root of these shapes.

2. Methods

2.1. General

In this research, three anchor models of different sizes were dragged over various surfaces on the beach and on the sea bottom, continuously measuring and recording the pulling force. An effort was also made to film the moving anchor models underwater.

However, some of these videos were of poor quality, because the visibility was significantly reduced by clouds of suspended sand particles caused by anchor movement.

2.2. The Anchor Models

In 1982, a sponge diver at Uluburun, near Kaş, on the Turkish southern coast, discovered a shipwreck on the rocky underwater slope. The shipwreck was excavated for over ten years by teams of archaeologists, primarily from Texas A&M University, led by Professor [11,12]. It was found that the ship carried a diverse load, including a cluster of 22 stone anchors with masses between 97 and 201 kg and 2 smaller anchors. It was dated by the cargo it carried to the end of the 14th century BCE.

Three anchor models were manufactured based on geometrical similitude to one of the Uluburun anchors (No. KW4589). The model anchors were made from slabs of quartz sandstone, a beach rock found along the Carmel coast in Israel, locally called *kurkar*, similar to that of the Uluburun anchors [13]. The mass density of samples of this rock was measured and found to be around 1720 kg/m^3 [10] The slabs were purchased from an authorized merchant, and hand-chiseled by A. Miller and colleagues, to create small, medium, and large anchors (Figures 1 and 2).

Figure 1. A. Miller hand-chiseling the large anchor (photo: M. Bram).

Figure 2. The anchor models (photo—N. Lavi).

The anchor weight in water is given by the following expression:

$$W = m * g * \left(1 - \frac{\rho_w}{\rho_s}\right) \quad (1)$$

where:

W—weight in water [N];
m—mass [kg];
g—gravitational constant (g = 9.81 m/s^2);
ρ_w—mass density of water (~1040 kg/m^3);
ρ_s—mass density of the stone (1720 kg/m^3).

As can be seen in Table 1, due to the buoyancy, the weight of the anchors under water is only about 40% of their weight in air. Therefore, what seems to be a very heavy anchor when handled on land, becomes only moderately heavy under water. This could have been a reason for the need for heavy and very heavy (in air) anchors for the Bronze Age ships [10].

Table 1. The main dimensions of the anchor models.

Anchor Model	Linear Scale Factor	Height [cm]	Width [cm]	Thickness [cm]	Mass [kg]	Weight [N] In Air	Weight [N] In Water
Uluburun KW4589	1:1	83	63	23	171	1677	663
Small	1:1.75	43	33	~12	32	314	124
Medium	1:1.33	54	42	~15.2	73	716	283
Large	1:1.11	69	52	~19.1	124	1216	481

2.3. Test Set-Up

The tests were conducted on a beach in Akko (Israel). They were instrumented with a load cell (Type 615 steel, capacity 500 kgf, made by Tedea-Huntleigh Electronics Co. Ltd., Cardiff, UK) measuring the force (in kg force—kgf) required to drag the anchor. The force was recorded at a rate of 2000 readings per second. The load cell and its electronic system were connected to the dragging winch via a pulley to keep the electronics dry (Figures 3 and 4). The recorded force had to be multiplied by 2 to obtain the actual force, because of the pulley in the system.

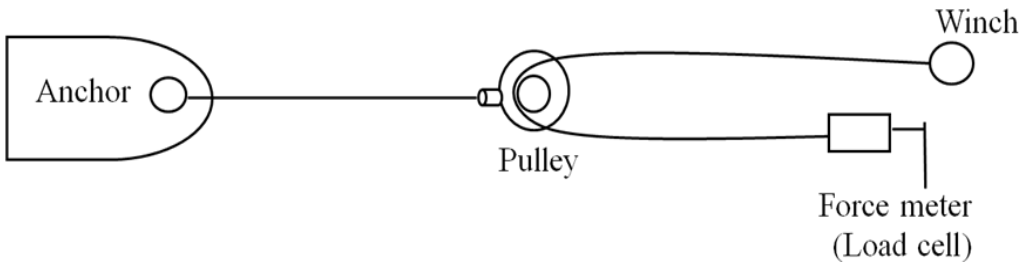

Figure 3. The setup for force measuring (drawing by A. Miller).

The recorded data included the timing of each data point (date, hour, minute, second, thousandth of a second), and the force measured at that point in time, in kilogram-force (1 kgf = 9.81 N). Because the force was measured and recorded in kgf, all the following data reduction was performed using this unit, but the final results were converted to the MKS unit system.

In addition to the force measurement, there was a setup for underwater video recording of the movement of the anchor. This included three cameras and a set of 'chess-board' markers to enable the observation of the anchor movement in the three axes. The photographic setup enabled calibration and automatic tracking of the motion. In addition, a strobe light was used to synchronize the video recording with the force measurement

recording (Figure 4). A special-purpose automatic photo-digitizing and processing software package based on Matlab® (Version 2016A) was designed and implemented by B.E. Karlin. The processed trajectory data show a rather constant and consistent speed beyond the initial acceleration stage.

Figure 4. The test set-up in Akko (photo: R. Levinson).

The winch characteristics were such that it pulled the anchor at an almost constant rate of 56 ± 2 mm/s with variable force, i.e., it exerted more or less force as required, to keep the anchor moving at that steady pace. The anchors were pulled for about 20–40 s, thus moving about 1–2 m.

The surfaces over which the anchors were pulled were practically flat and level, with less than 2° slope. The damp sand was the regular beach sand, totally drained after being washed by the waves. The dry sand was fine, sun-scorched, totally dry, and free-flowing. We assume that as long as the ratio of sand particle to the size of the specimen being dragged is in the 1/200 to 1/1000 range, with similar consistency of the particles, results of similar tests will have characteristics similar to those reported here. On dragging anchors over surfaces with different particle size range and consistency, additional physical processes may contribute to the measured force and somewhat alter its characteristics. The same reasoning applies to the sea bottom over which the anchors were pulled, which is practically level, with shallow undulations due to wave action and local currents.

A total of 84 dragging tests were carried out, 73 of them yielding useful data (Table 2). The tows were on different paths.

The last series of drags, dragging in an initial 30° upward direction, was run for preliminary assessment of the initial rotational behavior of the anchors. This series is discussed in [10] and is not relevant to this article. Excluding this series, there were 77 drags of the three anchors on four types of surface: dry sand, damp sand, sandy bottom, and rocky bottom, with an emphasis on the underwater surfaces. At a later stage, 10 more

long drags were added to estimate the range at which sand accumulation in front of the anchor reached a steady state (see Section 4.5).

Table 2. Summary of the drags performed.

Serial Number	Type of Surface	Anchor Mass [kg]	No. of Drags	Drags With Data
1	Dry sand	32	3	3
2	Dry sand	73	3	3
3	Dry sand	124	3	3
4	Damp sand	32	3	3
5	Damp sand	73	3	2
6	Damp sand	124	3	3
7	Sandy bottom	32	11	4
8	Sandy bottom	73	12 + 5 *	17
9	Sandy bottom	124	9 + 5 *	12
10	Rocky bottom	32	9	8
11	Rocky bottom	73	8	8
12	Dragging at 30°	73	7	7

* A total of 5 additional long drags, carried out (see Section 4.5).

Dragging the anchor models on each of the surfaces demonstrated different attributes of the force signal, indicating that a range of physical processes are at work, as shown and discussed below.

3. Results

3.1. The Recorded Force Signal

The load-cell that measures the force in the system actually measures the tension in the rope pulling the anchor. This means that the force record shows the initial tension build-up in the rope with all its components (the rope tied to the anchor, the pulley, the rope that goes around the pulley, one of its ends locked, and the other connected to the load cell) and the force exerted by the moving anchor on the rope. Figure 5 shows a typical signal, recorded while dragging the heavy anchor on damp sand on the beach. Various attributes of the force history are marked.

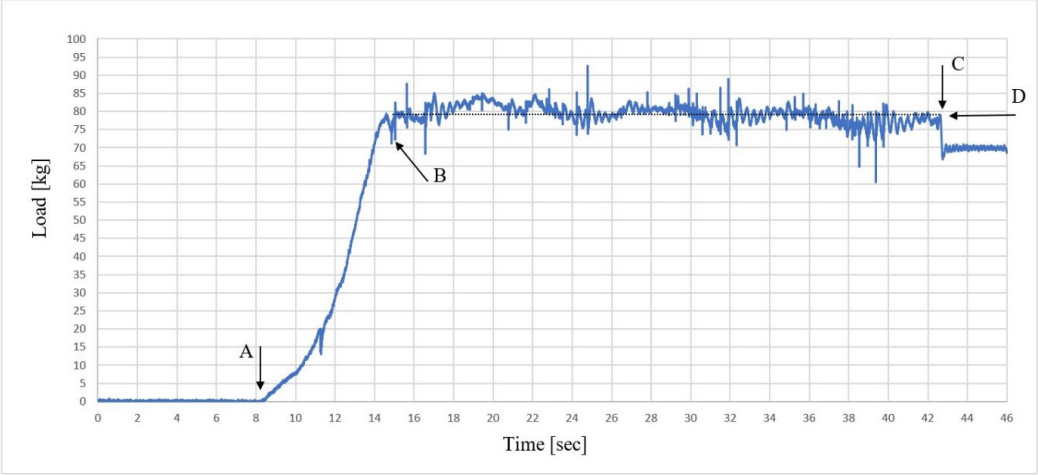

Figure 5. The attributes of the force signal of dragging the heavy anchor model on damp sand (on the beach). A—the beginning of the drag, beginning of stretching the rope. From A to B—stretching the rope with the tension rising in it. B—the beginning of the anchor movement. C—the end of the drag (the end of the anchor movement), partial release of the tension in the rope. D—the average force of dragging the anchor. From C to D—an almost constant force, indicating an almost steady state during the dragging.

The oscillations visible on the signal top, with about 0.3 Hertz frequency, are due to the string-like oscillations of the cable pulling the anchor.

As can be seen, the top of the signal (the B-to-C steady-state region) is rather smooth, and the average value of the force is a rather good representation of the force acting on the anchor throughout this drag. As shown later, the shapes of most of the signals recorded in this study are different from the shape of this particular force signal.

3.2. The Force-Type Groups

The recorded signals can be divided into six groups, each having a typical shape of the force record (Figure 6). These shapes (and not the force levels) attest to different physical processes involved in the anchor dragging.

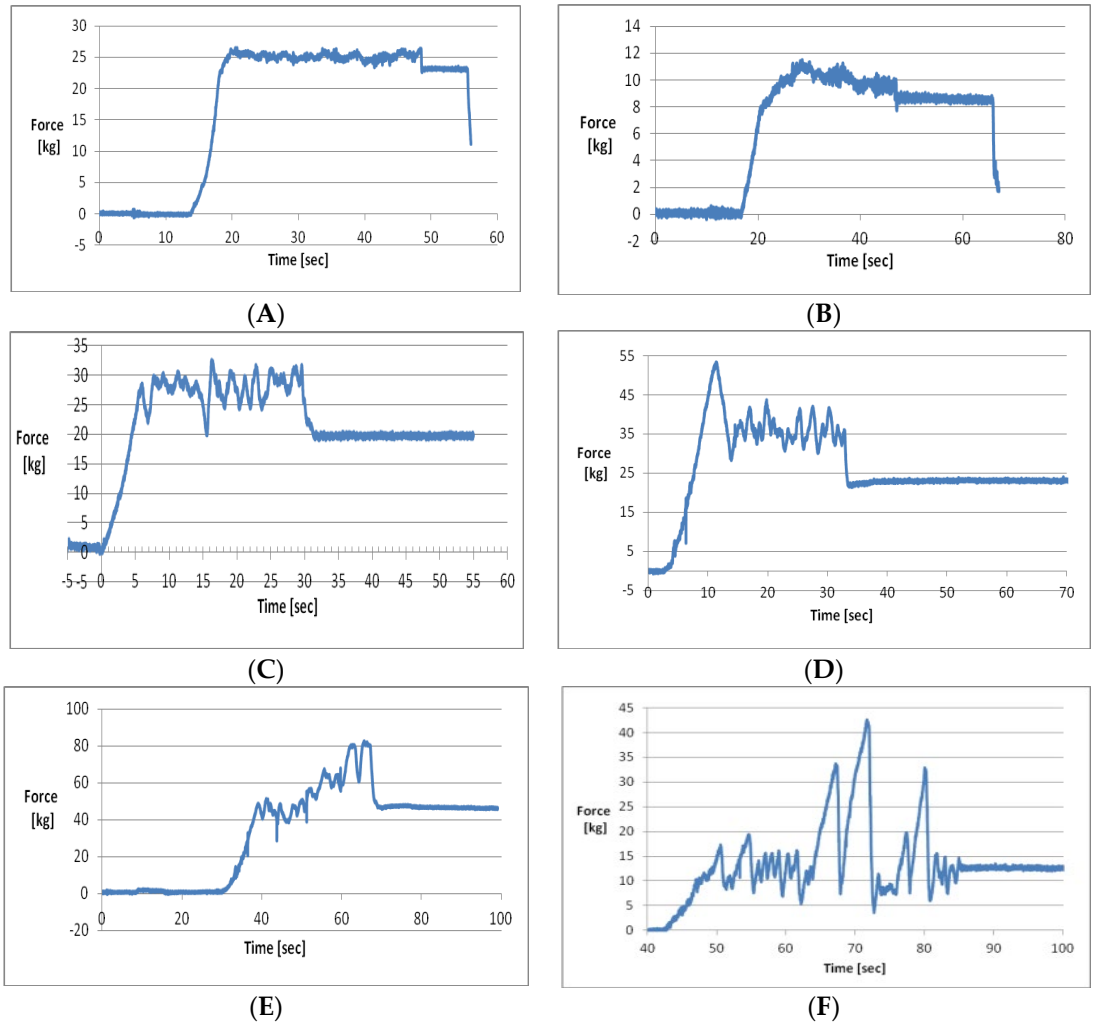

Figure 6. Representative types of force signals. Type (**A**)—flat top, indicating a constant dragging force with no disturbances (73 kg anchor on damp sand). Type (**B**)—relatively flat top with low-frequency disturbances (32 kg anchor on dry sand). Type (**C**)—a flat-top with high-frequency disturbances (73 kg anchor on sandy bottom). Type (**D**)—high initial peak followed by a significantly lower flat top (73 kg anchor on sandy bottom). Type (**E**)—initial relatively low force value, followed by an increasing ramp, either smooth or with high frequency, modulated with high-amplitude disturbances (124 kg anchor on sandy bottom). Type (**F**)—a seemingly flat top with high-frequency disturbances and with random, high-amplitude peaks (32 kg anchor on rocky bottom).

3.3. Type A

The flat top indicates a constant force dragging the anchor; therefore, it is very tempting to say that it is similar to the accepted notion of sliding friction. However, this tells only part of the story. The other part is told by the photographs of the event (Figure 7).

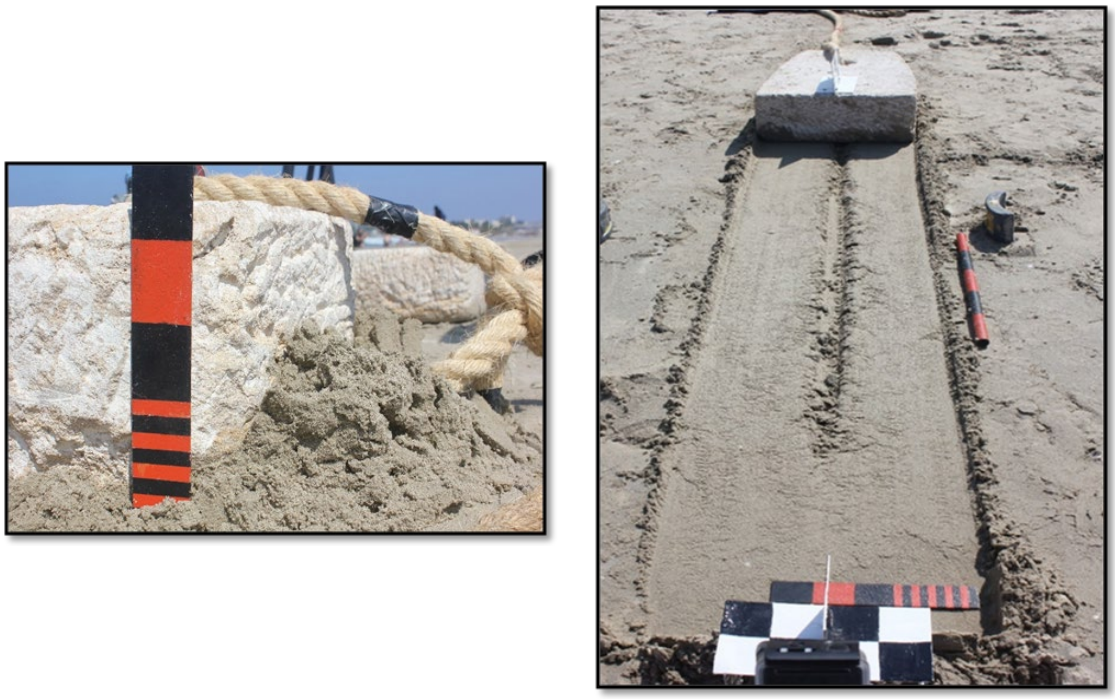

(**A**) (**B**)

Figure 7. Dragging the heavy anchor on damp sand. (**A**)—the sand accumulating in front of the anchor. (**B**)—the furrow plowed by the anchor in the top layer of the sand and the sand pushed from the front to both sides (photos: A. Yurman).

Figure 7A shows that sand was sheared off the top sand layer by the front of the moving anchor and accumulated at its moving front. Figure 7B reveals that the accumulated sand at the front was pushed sideways as the anchor moved forward. Hence, it seems that at least part of the measured force was actually the force required to shear off the top sand layer, for accelerating it to the anchor velocity and for pushing it sideways. Another part was the force required to smooth out the bottom of the furrow.

The top of the signal was flat because the surface on which the anchor was dragged was flat, in the first place. Had it been undulating, the shearing force would not have been constant and the force signal would have been undulating accordingly.

3.4. Type B

This is the realization of the process previously described, where the anchor was dragged on a non-flat surface of the dry sand on the beach. The amount of accumulated sand in front of the anchor varies, and so does the force required to drag the anchor and the varying amount of sand.

Since the signal is of the light model being dragged, the force amplitude is relatively low; however, the noise level is of roughly the same amplitude as in the previous signal, hence the signal only seems to have a more significant noise level.

3.5. Type C

This is the equivalent of Type A or B, only over a sandy surface under water. The relatively large amplitude of the high-frequency vibrations is typical to all the underwater

drags, and is probably the result of the front of the anchor pushing forward small quantities of saturated sand that easily flow sideways. The variation in the frequency and the amplitude could be the result of local variations in the flow properties of the sand (i.e., its consistency) and of the uneven surface over which the anchor moved.

3.6. Type D

This is an example of the liquefaction phenomenon [14,15]. The pressure of the anchor on the sand below it squeezed some of the water out of it, thus, creating a multitude of sand particle bridges and simultaneously water bridges by capillary attraction, strong and stable enough not only to support the anchor, but also to give the sand a significant shear strength. Pulling the anchor applied shear stress to these bridges, stronger than their shear strength, shattering the whole structure of the bridges. The previously expelled water seeped back in and the sand lost its supporting capabilities. However, instead of sinking further into the sand the anchor was pulled forward, shearing the sand in front of it and pushing it forward and sideways, as described above.

3.7. Type E

The anchor sank rather deeply into the sand so that the accumulating sand at its front added a significant mass to be pulled, in addition to the anchor itself. The increasing force indicates an increase in practically all the components of the force as the anchor was being pulled forward.

However, the sand cannot accumulate indefinitely. Apparently, the drags reported so far did not reach a steady state, where the amount of accumulated sand per unit time is equal to the amount pushed sideways, and the force graph becomes relatively flat.

This type of behavior was observed only with the 73 kg anchor (2 of 12 drags) and with the 124 kg anchor (all 9 drags). None was observed with the 32 kg anchor.

Assuming that the above proportions are representatives of the probability of the population of stone anchors to accumulate sand up front, this yields the graphs in Figure 8.

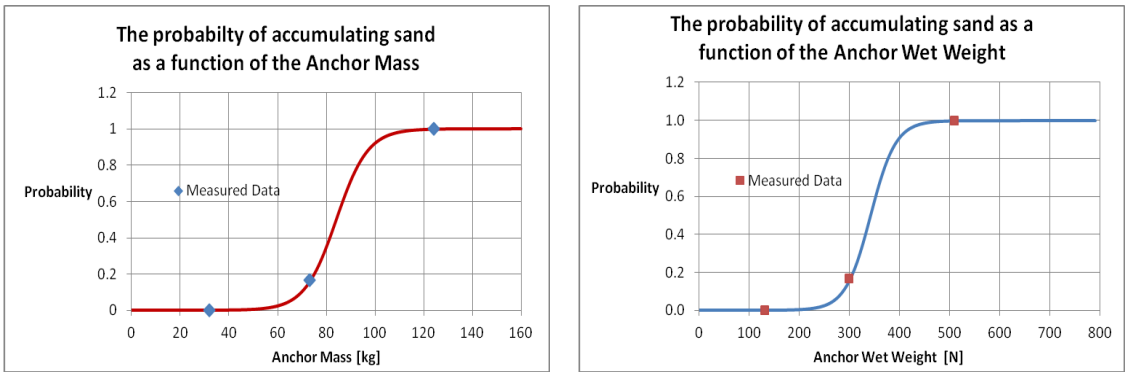

Figure 8. The probability of accumulating sand as a function of the anchor size.

Of course, for different sites with different types of sand, the results of such drags can be somewhat different and so will be the following plots.

The line fitted to the data is of the type:

$$P = 1/(1 + A \times \exp(-(W - B)/C)).$$

where:

P is the probability;
W is the mass or weight of the anchor (in air or in water);
A, B, C—constants.

It is suggested that the crew of a ship preferred an anchor that produced the maximum holding power at minimum weight, so they probably preferred anchors that accumulate as much sand as possible, i.e., anchors of above 100 kg mass.

To try and observe the transition to the assumed 'steady state', we carried out two sets of 'long' drags, each set of five drags, with the 73 and 124 kg anchors. In these drags, the anchors travelled 6 to 8 m, which allowed them to reach the assumed steady state.

As can be seen in Figure 9, the initial dragging force was around 44 kgf, rising to a steady state of around 57 kgf, with large fluctuations at three frequencies. The lower frequency is probably due to the wavy sand surface, the medium frequency is probably due to the rope vibrations, and the highest frequency is probably due to variations in the sand flow properties. Therefore, it seems that the 'steady state' is not so steady.

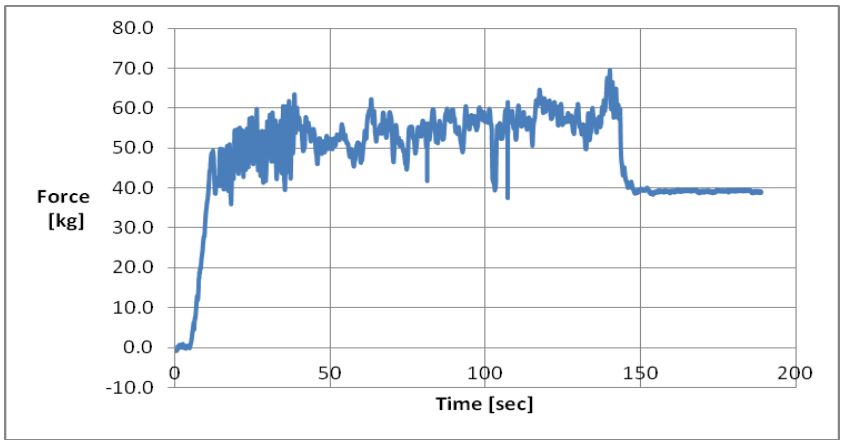

Figure 9. A long drag of the 124 kg anchor.

The initial dragging force of around 44 kgf was the average for all the drags of the 124 kg anchor, which weighed 51.9 kgf underwater (see Table 3). That is, a force of 44 kgf was required to drag the 51.9 kgf anchor, therefore, 57 kgf force (the average force at the top of the ramp) could drag about 67 kgf, i.e., about 15 kgf of added sand burden, or about 30% additional weight.

Table 3. Effective coefficient of friction for the initial movement of the anchor.

Surface	Anchor Weight [N]	Average Dragging Force [N]	Effective Coefficient of Friction	Average per Surface Type
Dry sand	314	218	0.69	0.65 ± 0.06
Dry sand	716	483	0.67	
Dry sand	1216	783	0.64	
Damp sand	314	205	0.65	0.68 ± 0.03
Damp sand	716	499	0.70	
Damp sand	1216	856	0.70	
Sandy bottom	131	114	0.87	0.86 ± 0.08
Sandy bottom	299	273	0.91	
Sandy bottom	509	404	0.79	
Rocky bottom	131	133	1.01	1.11 ± 0.09
Rocky bottom	299	361	1.20	

The weight of the anchors underwater is reduced (relative to in air) due to the buoyancy. The forces measured in the tests were in kgf and are translated here to Newtons.

3.8. Type F

This type of force record is typical to the measured force of the drags over the rocky surface. Such a rocky underwater surface is never really smooth. It always has crevices and protrusions, either on a single rock surface or on a cluster of rocks. In fact, the movement of an anchor over a rocky surface is quite similar to running an obstacle course. This is demonstrated in Figure 10, with the 32 kg anchor being dragged over what is considered a smooth rock surface.

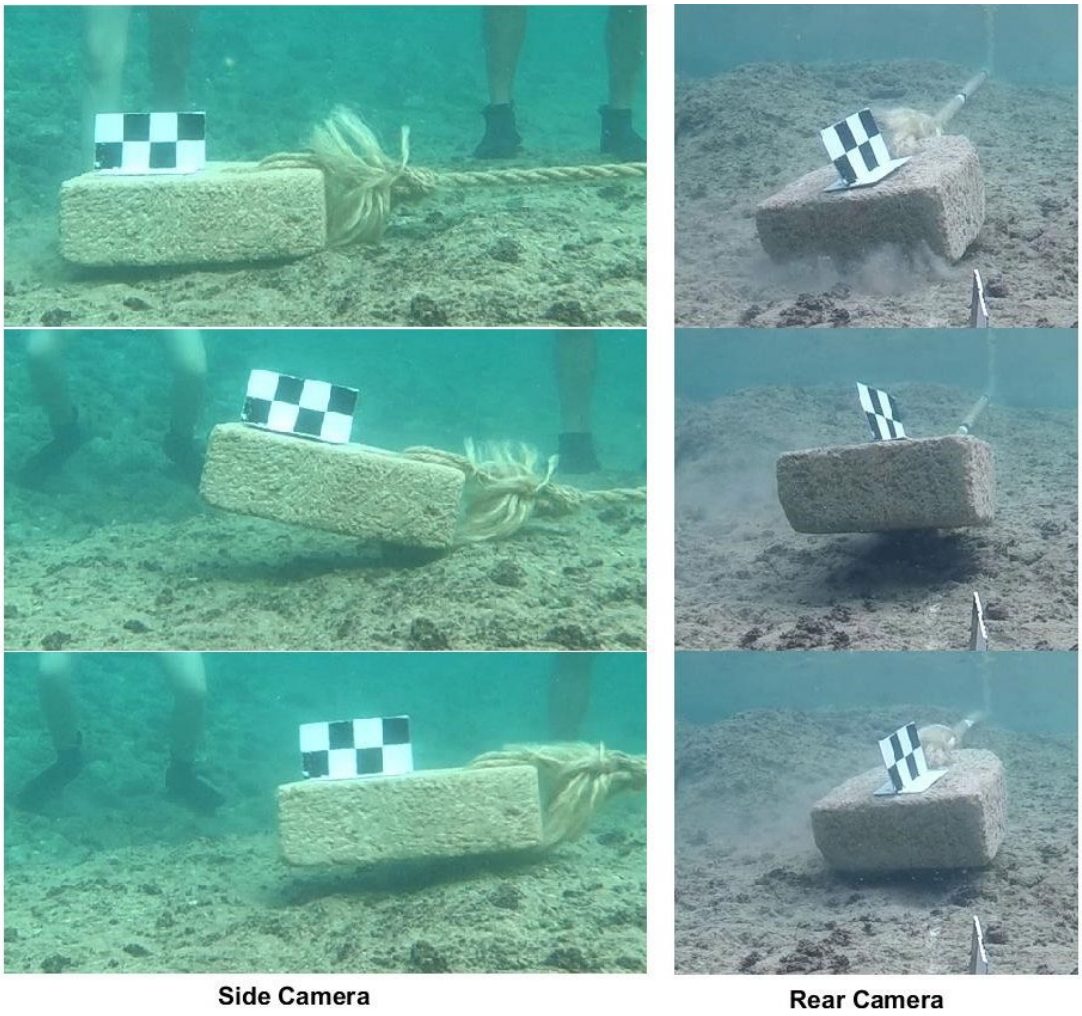

Figure 10. The 32 kg anchor encountering a small protrusion on the surface of the rock, producing a spike in the force record (the time runs from the top down). (Photos: B. E. Karlin).

Given the winch specifications (Section 3 above), such an occurrence obviously causes a spike in the force graph. Since the distribution of such disturbances along the anchor's trajectory is random, so is the occurrence of these spikes in the force record.

4. The Physical Processes Involved

4.1. Anchor Sinking in the Sand

When an anchor of a given weight and a given face area is laid on the sand surface, below it is a mixture of sand and air, or sand and water (under water), or a mixture of all three (on the beach). The weight of the anchor causes it to sink into the surface, thus, compressing the mixture under it. The sinking depth depends on the compression load imparted by the anchor, on the condition of the sand (saturated, wet, dry), on its ability to flow, and on its ability to form mini-bridges capable of supporting a load, i.e., on the consistency and average shape of the sand particles.

Therefore, the anchor sinks to a depth at which it is supported by the microstructure of the sand, created by the loading and the drainage of part of the flowing phases (water, air) from among the solid components, creating a structure, sufficiently strong to support the external load.

4.2. Sand Shear Strength

The microstructure created by the compressive load has some shear strength. When the anchor is pulled by the rope, it creates a shear stress on the surface between the anchor

bottom and the top layer of the sand. When the pull is sufficiently strong and exceeds this shear strength, the anchor begins to move. The beginning of the anchor movement breaks the sand microstructure that supported it, the water takes over, and the saturated sand returns to its flowing condition.

The force required to begin the movement is, therefore:

$$F_{shear} = \tau_{interface} A_{anchor} \quad (2)$$

where:

F_{shear} [N] is the force required to shear the interface at the locations supporting the anchor, to allow the anchor to move;
$\tau_{interface}$ [Pa] (=[N/m^2]) is the shear strength of the interface.

4.3. Shearing the Sand by the Anchor

It is assumed here that the process is at a steady state.

Once the anchor begins to move, it has to shear off the sand at its front. This sand was not compressed by the sinking, so that its shear strength is lower than that of the anchor–sand interface. In the tests, the pull was at a constant velocity of ~56 mm/s so that a sand mass was continuously added to the anchor, at a rate of about:

$$dm_{added}/dt = \rho_s L h V \quad (3)$$

where:

ρ_s [kg/m^3] is the mass–density of the sand at that particular location with the other phases included;
L [m] is the length of the anchor front;
h [m] is the depth to which the anchor sank;
V [m/s] is the pulling velocity (in our case: 0.056 m/s).

4.4. Sheared Sand Acceleration

Once this mass is sheared off, it is accelerated to the velocity of the anchor by a process of compression and release. As yet, there is no physical estimate regarding the acceleration time, but we know it is different at different conditions and mixtures of the sand. The forward acceleration of the sand requires a certain force $F_{forward}$, which is constant at a steady state.

4.5. Accumulating Sand in Front

The pull velocity is constant and mass is continuously added in front of the anchor. This cannot continue endlessly, as the accumulated mass at the anchor front cannot increase beyond a certain limit. This limit is not known; however, at a steady state, the rate at which mass is added to the anchor front equals the rate at which mass is pushed to the sides of the anchor, to create a furrow. This pushing of the sand sideways requires additional force $F_{sideways}$, also of unknown magnitude.

4.6. Effective Coefficient of Friction

As the anchor begins to move, it slides over the area that was sheared off during the previous stages of movement. Since this sliding is of a solid anchor over a somewhat compacted and practically level surface, it can be assumed that the force required for this sliding can be estimated by using the classical friction relation:

$$F_{friction} = \mu W_{anchor} \quad (4)$$

where:

μ [-] is the coefficient of friction;
W_{anchor} [N] is the weight of the anchor, in air or water (as given by (Equation (1))) acting in a direction normal to the interface.

Therefore, the force required to drag the anchor over the sand surface is the sum of all the above partial forces. Until further work is performed to evaluate each of these forces, it is possible to use an effective coefficient of friction, either for those cases where the force plot is relatively flat, or to estimate only the coefficient of friction at the beginning of the anchor movement, realizing that it is not applicable to the other phases of the drag (Table 3).

5. Discussion

5.1. Friction

It is evident that dragging a stone anchor on sand or natural rock surface is totally different from the classical rigid, relatively smooth bodies sliding over each other. It involves different physical processes. It is not only a surface phenomenon, since bulk material properties come into play in the interaction between the anchor and the surface it is being dragged over.

However, although the conventional coefficient of friction is not applicable here, there are several situations where the dragging force is practically constant (a combination of shear force and sand moving), for which an effective coefficient of friction can be used. In these cases, it has to be noted that the value of this coefficient cannot be used for other cases and applications.

In a simplistic way of describing the process until a steady state is reached, it can be assumed that an effective coefficient of friction μ* is at work, so that the frictional force can be written as:

$$F_{friction} = \mu^{*} F_{normal} = \mu^{*} W_{anchor} \tag{5}$$

where:

$F_{friction}$ is the frictional force required to move the anchor over the flat sand surface;
W_{anchor} is the weight of the anchor in air or water (depending on where it is during the drag). This weight includes the weight of the sand accumulating at the front of the anchor.

The value of the effective coefficient of friction depends on the weight of the anchor, as explained in Section 4, above. This can be written as:

$$\mu^{*} = \mu^{*}(W_{anchor}) \tag{6}$$

Therefore, the variation of the frictional force (as seen in the force plot) is:

$$\frac{dF_{friction}}{dt} = W_{anchor}\frac{d\mu^{*}}{dt} + \mu^{*}\frac{dW_{anchor}}{dt} \tag{7}$$

The derivative of μ* is (by the chain rule):

$$\frac{d\mu^{*}}{dt} = \frac{d\mu^{*}}{dW_{anchor}}\frac{dW_{anchor}}{dt} \tag{8}$$

Hence, expression (7) obtains the form:

$$\frac{dF_{friction}}{dt} = W_{anchor}\frac{d\mu^{*}}{dW_{anchor}}\frac{dW_{anchor}}{dt} + \mu^{*}\frac{dW_{anchor}}{dt} \tag{9}$$

$$= \left(W_{anchor}\frac{d\mu^{*}}{dW_{anchor}} + \mu^{*}\right)\frac{dW_{anchor}}{dt} \tag{10}$$

Obviously, the weight of the anchor itself does not vary with the drag, but the dragged mass does change with the accumulation of sand at its front, and occasionally also on top of the anchor itself. This is partly given by expression (3) above.

$$\begin{aligned}\frac{dF_{friction}}{dt} &= \left(W_{anchor}\frac{d\mu^{*}}{dW_{anchor}} + \mu^{*}\right)\frac{g*dm_{added}}{dt} \\ &= \left(W_{anchor}\frac{d\mu^{*}}{dW_{anchor}} + \mu^{*}\right)g\rho_{s}Lhv\end{aligned} \tag{11}$$

The problem here is that expression (6) is still an unknown.

As already mentioned, it is sometimes possible to use the 'effective coefficient of friction' to estimate the holding power of a given anchor. A list of these coefficients, as measured in this research is given in Table 3, above. According to the data in Table 3, the coefficient of friction of the stone anchor over a rocky surface is about 30% higher than over sandy bottom. This means that if an anchor of 100 kg mass is sufficient to hold a certain ship in place over a sandy bottom, then over a rocky surface, a 70 kg anchor may suffice, and this means easier handling of the anchor on board the ship and reduced risk to the crew.

5.2. Anchor Sinking

A parameter, only mentioned above, is how deeply the anchor sinks into the sand. It appears that the longer the anchor stays in place, the deeper it sinks, and, hence, the thicker the sand layer pushed forward, the sand accumulation at the anchor's front, and consequently the shape of the force record.

The longer the stay, the more water is squeezed out and drained from below the anchor, the more compressed the sand becomes, meaning that more sand bridges and capillary bridges are formed, so that the sand shear strength increases, probably in asymptotic convergence to a steady state. As described above, this has implications on the force required to move the anchor from its location. Under specific sets of conditions, this may result in the liquefaction of the sand under the anchor and the sudden reduction in its shear strength.

5.3. Vertical Movement of the Anchor

So far, it has been assumed that all the movements of the anchor are in the horizontal plane, but this is not always the case. It happens occasionally that the front of the anchor climbs over the accumulated sand at its front. At a certain point of the dragging, the center of gravity of the anchor goes ahead of the sand 'hill', so that its front drops and digs into the sand further in front, thus, beginning a sequence of vertical oscillations.

A similar effect can be the result of the string-like vibrations of the tight pulling rope, particularly with light anchors, where the mass of the length of the rope is similar to or higher than that of the anchor itself. In such a case, although the rope does not add to the force required to move the anchor (it floats and has a negligible drag), the rope vibrations might cause the light anchor to hop over considerable stretches of ground, when the anchor holding power diminishes to zero.

Another cause of vertical movement can be that the dragging vector may be oblique with an oscillatory mechanism caused by wave action and/or the ship's movement. Hence there are several possible causes of vertical movement of an anchor, but this is out of the scope of this article.

5.4. Variability

In this work, over 70 force records with different attributes were produced, and related to various physical processes. The underwater drags on sandy seafloor were carried out in the same location, having similar sea and wave conditions. The drags over rocks were also carried out over a rock surface at a different site on different paths. It must be kept in mind that at different locations, with different types of sand, different rocks, and with different currents and wave conditions, the force records may change, resulting in different shapes of force records and different interpretations.

The variations in these conditions are particularly pronounced in shallow water. Stone anchors were used primarily during the Bronze and Iron Ages, when shipping was essentially coastal, in relatively shallow water, and, thus, prone to the above-mentioned variations.

Captains, then like now, were primarily concerned with the safety of their vessels and crews, hence, they always took precautions, which, based on the above, means the use of heavy anchors. However, manual handling of the heavy anchors posed a risk both to the ship and to the crew [10], so that the captains had to choose their preferences, an incentive to develop more effective anchors.

5.5. Actual Anchor Dragging

It is important to note that the tests reported here simulate actual dragging of the anchor only when the ship itself is securely tied and cannot move. When the ship is loose, pulling the anchor rope moves both anchor and ship. They become closer to each other, until the pulling point on the ship is situated right over the anchor. This process happens no matter what level of force is required to drag the anchor (when the ship is tied). When the pulling point on the ship is altered, this can be used to direct the ship to point to the desired direction, together with having the anchor right under the crane, derrick, or any other means for hoisting the anchor on board.

When the anchor is locked on the bottom, among rocks or due to any other cause, pulling the anchor rope moves only the ship until it is situated right over the anchor (or any other locked point along the rope). If the anchor cannot be set free, the rope has to be cut to enable the ship to sail away. Similarly, if the crew cannot manage to raise a heavy anchor, the rope has to be cut and the ship set loose. The anchor remains on the bottom and the ship has to use another anchor, kept on board in reserve.

When the anchor is dropped, the length of the rope has to be significantly longer than the actual depth, to allow for horizontal and vertical movements of the ship, due to currents and waves motions. Therefore, the process described above is repeated on each entering and leaving an anchorage.

It is interesting to note that similar processes and results are encountered on erecting the mooring for floating offshore wind turbines, using modern shape anchors [16].

6. Summary and Conclusions

Extensive research was carried out regarding the holding power of Mediterranean stone anchors during the Bronze and Iron Ages. Anchor models of three sizes were produced and dragged over dry and damp sand on the beach, on a sandy sea bottom, and a rocky surface under water. All these drags included measuring and recording of the force required to drag the anchors.

The force records have common attributes, but can also be divided into several groups, each group having common additional attributes that can be related to the physical processes involved in the drags of that group. On a sand surface, these processes include the increase in the sand shear strength due to the pressure imposed by the anchor, shearing the sand in front of the anchor, accelerating it to the anchor velocity, adding the mass of the accumulated sand to that of the moving anchor, and pushing part of the accumulated sand sideways. All these are in addition to the force required to overcome the friction between the anchor face and the sand surface.

On a rocky surface, in addition to the friction between the anchor face and the rock surface, there is the encounter between the anchor front and rocky protrusions.

The mere presence of all the processes listed above attests to the fact that the force measured and recorded is markedly different from the regular, sliding frictional force, represented by expression (5) above. In reality, it is much more complex, and expressing it properly requires additional work to characterize sand properties at various levels of saturation, to measure the dependence of the sand load-carrying capabilities, and of the shear strength on the pressure exerted by the anchor.

Author Contributions: Conceptualization and methodology, Y.M.-B.; software, B.E.K.; Investigation, resources and project administration A.M. and D.C.; visualization B.E.K.; writing, review and editing, Y.M.-B.; supervision D.C. All authors have read and agreed to the published version of the manuscript.

Funding: This project was financially supported by a Sir Maurice Hatter Fellowship.

Institutional Review Board Statement: Not applicable.

Informed Consent Statement: Not applicable.

Data Availability Statement: Data are contained within the article.

Acknowledgments: The authors express their appreciation and thanks to C. Pulak for his kind permission to reproduce one of the Uluburun anchors; A. Yurman and M. Bachar from the Maritime Workshop of the Leon Recanati Institute for Maritime Studies and E. Itzhack for their valuable assistance and support in executing this project; all the volunteers who participated in the field work, out of interest and comradeship; and J. B. Tresman for the English editing. Special thanks are due to the anonymous reviewers, the editor and the editorial staff. The article is dedicated to the memory of our colleague, friend, and mentor, the late Yaacov (Yak) Kahanov, who suggested studying the characteristics of stone anchors.

Conflicts of Interest: The authors declare no conflict of interests.

References

1. Frost, H. The Stone Anchors of Ugarit. In *Mission de Ras Shamra XVII. Ugaritica VI*; Librairie Orientaliste P. Geuthner: Paris, France, 1969; pp. 235–245.
2. Frost, H. The Stone Anchors of Byblos. In *Mélanges de l'Université Saint-Joseph LXV*; Librairie Orientaliste P. Geuthner: Paris, France, 1969; Volume 26, pp. 425–442. [CrossRef]
3. Frost, H. Bronze-Age Stone-Anchor from the Eastern Mediterranean. Dating and Identification. *Mar. Mirror* **1970**, *56*, 377–394.
4. Frost, H. Ports, Cairns and Anchors. A Pharaonic Outlet on the Red Sea. *Topoi. Orient-Occident* **1996**, *6*, 869–902. [CrossRef]
5. Wachsmann, S. *Seagoing Ships and Seamanship in the Bronze Age Levant*; Texas A&M University Press: College Station, TX, USA, 1998.
6. Votruba, F.G. Building upon Honor Frost's Anchor-Stone Foundations. In *In the Footsteps of Honor Frost: The Life and Legacy of a Pioneer in Maritime Archaeology*; Blue, L., Ed.; Sidestone Press: Leiden, The Netherlands, 2019; pp. 213–244.
7. Galili, E.; Sharvit, J.; Artzy, M. Reconsidering Byblian and Egyptian stone anchors using numeral methods: New finds from the Israeli coast. *Int. J. Naut. Archaeol.* **1994**, *23*, 93–107. [CrossRef]
8. Kapitän, G. Ancient Anchors—Technology and Classification. *Int. J. Naut. Archaeol.* **1984**, *13*, 33–44. [CrossRef]
9. Curryer, B.N. *Anchors: An Illustrated History*; Naval Institute Press: Annapolis, MD, USA, 1999.
10. Miller, A.; Cvikel, D.; Me-Bar, Y. The Holding Power of Bronze Age Stone Weight Anchors. *Skyllis* **2018**, *18*, 224–227.
11. Pulak, C. The Uluburun Shipwreck: An Overview. *Int. J. Naut. Archaeol.* **1998**, *27*, 188–224. [CrossRef]
12. Pulak, C. The Uluburun Shipwreck and Late Bronze Age Trade. In *Beyond Babylon: Art, Trade and Diplomacy in the Second Millennium B.C.*; Aruz, J., Benzel, M., Evans, J.M., Eds.; The Metropolitan Museum of Art: New York, NY, USA; Yale University Press: New Haven, CT, USA; London, UK, 2008; pp. 289–310.
13. Goren, Y. International Exchange during the Late Second Millennium B.C. Microarchaeological Study of Finds from the Uluburun Ship. In *Cultures in Contact. From Mesopotamia to the Mediterranean in the Second Millennium B.C. (New York 2013)*; Aruz, J., Graff, S.B., Rakic, Y., Eds.; Yale University Press: New Haven, CT, USA, 2013; pp. 54–61.
14. Heider, Y. Saturated Porous Media Dynamics with Application to Earthquake Engineering. Report No. II-25. Ph.D. Thesis, Institut für Mechanik (Bauwesen), Lehrstuhl für Kontinuumsmechanik, Universität Stuttgart, Stuttgart, Germany, 2012.
15. Zhou, C.; Zheng, S.; Ye, Y.; Wang, H. Review on Seismic Liquefaction of Seabed Soil. *IOP Conf. Ser. Earth Environ. Sci.* **2019**, *310*, 042052. [CrossRef]
16. Dao, D.A.; Dicke, K.; Grabe, J. Investigation of anchor installation for floating offshore wind turbines. In Proceedings of the 10th International Conference on Physical Modelling in Geotechnics, Daejeon, Republic of Korea, 19–23 September 2022.